ROBOTIC SYSTEM FOR ACTIVE DEBRIS REMOVAL: REQUIREMENTS, STATE-OF-THE-ART AND CONCEPT ARCHITECTURE OF THE RENDEZVOUS AND CAPTURE (RVC) CONTROL SYSTEM

July 14, 2015

Marko Jankovic
German Research Center for Artificial Intelligence (DFKI) and University of Bremen
Early Stage Researcher and PhD Student
Robert-Hooke-Str. 1, 28359, Bremen, Germany
marko.jankovic@dfki.de
Kartik Kumar (Dinamica Srl), Natalia Ortiz Gomez (Southampton University), Juan Manuel Romero Martin (Strathclyde University), Frank Kirchner (German Research Center for Artificial Intelligence (DFKI)), Francesco Topputo (Politecnico di Milano), Scott J. I. Walker (Southampton University), Massimiliano Vasile (Strathclyde University)

ABSTRACT

Recent studies of the space debris population in Low Earth Orbit (LEO) have concluded that certain regions have likely reached a critical density of objects, which could eventually lead to a cascading process known as the Kessler syndrome. Thus, the growing perception is that we need to consider Active Debris Removal missions (ADR) as an essential element to preserve the space environment for future generations. Among all objects in the current LEO environment, Ariane rocket bodies (R/Bs) are some of the most suitable targets for future robotic ADR missions, given their number, mass properties and spatial distribution. ADR techniques involving orbital robotics are considered relatively well-understood options, since technologies and theories for automated robotic capture and servicing of spacecraft already exist and have undergone successful in-orbit testing. However, rendezvous and capture of large, non-cooperative objects is a highly challenging task, especially with a robotic system. In fact, at present, the technologies necessary for proximity operations and capture, even of controlled targets, lack in maturity. Therefore, to enable future robotic ADR missions there is a pressing need for more advanced and modular systems that can cope with non-controlled, tumbling objects.

The rendezvous and capture (RVC) control system is one of the most critical subsystems of future robotic ADR missions. Within that context, we present a concept of a robotic spacecraft capable of approaching, capturing and manipulating R/Bs. Moreover, we provide a more detailed overview of the envisioned control architecture, bearing in mind the requirements for the most critical phases of an ADR mission, which are the close-range rendezvous and final approach. The modules of the RVC control architecture covered by our work include the: navigation module, guidance module, control module, de-tumbling module and robotics module. Each module is responsible for particular functions within the overall system, which are illustrated in this paper. The target is assumed to be non-cooperative, although its shape is well-characterized a priori. We provide a synopsis of the challenges that proximity operations pose for the design of a robotic RVC control system for ADR.

Nomenclature

Acronyms

ACS *Attitude Control System*

ACT *Attitude Control Thruster*

ADCS *Attitude Determination and Control System*

ADR *Active Debris Removal*

Agora *Active Grabbing & Orbital Removal of Ariane*

CAM *Collision Avoidance Maneuver*

CMG *Control Moment Gyro*

COG *Center of Gravity*

DMC *Distributed Momentum Control*

EE *End-Effector*

EKF *Extended Kalman Filter*

ETS *Engineering Test Satellite*

FDIR *Failure Detection, Isolation and Recovery*

GJM *Generalized Jacobian Matrix*

GNC *Guidance, Navigation and Control*

HEO *High Earth Orbit*

HTS *High Temperature Superconducting*

IMU *Inertial Measurement Unit*

LEO *Low Earth Orbit*

LHP *Loop Heat Pipe*

LQR *Linear-Quadratic Regulator*

MEO *Medium Earth Orbit*

MILP *Mixed-Integer Linear Programming*

MIMO *Multiple-Input-Multiple-Output*

MVM *Mission Vehicle Management*

OCT *Orbital Control Thruster*

OE *Orbital Express*

OOS *On-Orbit Servicing*

PID *Proportional-Integral-Derivative*

PMD *Post-Mission Disposal*

R/B *Rocket Body*

RVC *Rendezvous and capture*

RW *Reaction Wheel*

SISO *Single-Input-Single-Output*

SRMS *Shuttle Remote Manipulator System*

UKF *Unscented Kalman Filter*

VEB *Vehicle Equipment Bay*

Abbreviations

DEOS *Deutsche Orbitale Servicing mission*

EPS *Storable Propellant Stage*

Symbols

$\dot{\boldsymbol{\phi}}_m$ Angular velocity of joints of the manipulator, [rad/s]

$\dot{\boldsymbol{\phi}}_r$ Angular velocity of CMGs, [rad/s]

ΔV Velocity change of the spacecraft, [m/s]

$\dot{\boldsymbol{x}}_{gh}$ Velocity of the center of gravity of the robot projected onto the velocity of the end-effector, [m/s]

h Altitude of an object, [km]

$\boldsymbol{H}_b$ Augmented inertia matrix of the base, $[\mathrm{kg} \cdot \mathrm{m}^2]$

$\boldsymbol{H}_c$ Augmented coupling inertia matrix, $[\mathrm{kg} \cdot \mathrm{m}^2]$

$\boldsymbol{J}_m^*$ Generalized Jacobian Matrix for joint variables

$\boldsymbol{J}_r^*$ Generalized Jacobian Matrix for CMGs variables

$\boldsymbol{J}^*$ Generalized Jacobian Matrix

$\boldsymbol{L}$ Angular momentum of the spacecraft, $[\mathrm{kg} \cdot \mathrm{m}^2/\mathrm{s}]$

$\boldsymbol{L}_g$ Total angular momentum of the spacecraft around its center of gravity, $[\mathrm{kg} \cdot \mathrm{m}^2/\mathrm{s}]$

$\boldsymbol{\omega_b}$ Angular velocity of the base, [rad/s]

$\boldsymbol{\omega}_h$ Angular velocity of the end-effector, [rad/s]

$\boldsymbol{P}$ Linear momentum of the spacecraft, $[\mathrm{kg} \cdot \mathrm{m}/\mathrm{s}]$

$\boldsymbol{r}_g$ Position of the center of gravity of the robotic spacecraft, [m]

$\tilde{\boldsymbol{H}}_{bm}$ Modified augmented coupling inertia matrix between the base and manipulator, $[\mathrm{kg} \cdot \mathrm{m}^2]$

$\tilde{\boldsymbol{H}}_{br}$ Modified augmented coupling inertia matrix between the base and the CMGs, $[\mathrm{kg} \cdot \mathrm{m}^2]$

$\boldsymbol{v}_h$ Linear velocity of the end-effector, [m/s]

1 INTRODUCTION

Active debris removal is a burgeoning area of research, having gained prominence in recent years due to the mounting risk of on-orbit collisions. The space debris population has grown significantly over the last two decades, especially in Low Earth Orbit (LEO), leading to a sizable risk to operational satellites [1]. There is mounting concern in the community that the volume of debris objects is rapidly approaching, if not already beyond, the threshold predicted for the onset of the Kessler Syndrome [2]: a collisional cascade that could render certain orbital bands unusable in the future. Thus, to stabilize the space debris environment, there is growing consensus that this cannot be achieved solely through passive means, e.g., safely retiring currently-operational satellites at end-of-life. Active Debris Removal (ADR) may be necessary.

On the basis of this hypothesis, we study a rendezvous and capture (RVC) control system for a robotic mission concept to remove Ariane rocket bodies (R/Bs). Orbital robotics is an evolving field with significant heritage technology. Hence, a robotic capture concept is considered a viable option for ADR that requires further investigation. We study the RVC system in the context of the Agora mission: a technology demonstrator geared towards testing the feasibility of robotic capture of the Ariane upper stage used to place the chaser spacecraft on orbit. In addition, Agora also employs an active, contactless de-tumbling system based on eddy currents. We investigate the impact of the de-tumbling and robotic capture modules on the design of the overall RVC system.

In this paper, we present an overview of the concept being studied and focus on the RVC architecture needed to safely de-tumble, capture and manipulate the target object. In particular, we detail the mission requirements and constraints that impact the design of the Guidance, Navigation and Control (GNC) system on-board the chaser spacecraft. In Section 2, we present a short overview of the space debris problem. Subsequently, in Section 3 we present a summary of the state-of-the-art in robotic rendezvous and capture. Our reference mission, Agora (Active Grabbing & Orbital Removal of Ariane), is described succinctly in Section 4. We provide an overview of the top-level requirements of the mission and brief descriptions of the target and the chaser spacecraft. In addition, we provide a synopsis of the key mission phases, which feed into the design of the RVC control system. In Section 5, we introduce the main modules of the RVC control system and offer insight into constraints implied by the Agora mission. In particular, we describe the envisioned architecture for the GNC modules. We also take a closer look at the operation of the de-tumbling and robotic capture modules, with a view towards elucidating the general design framework. Finally, in Section 6, we summarize our main conclusions and outline our future work.

2 SPACE DEBRIS

Currently, the number of tracked space debris objects larger then 10 cm exceeds 29,000 [3] and each of them has the potential to catastrophically damage an operational spacecraft and generate further debris. To avoid this, collision avoidance maneuvers (CAMs) are generally performed. CAMs are becoming increasingly frequent [4] highlighting the rising threat of space debris.

The risk metrics used to identify targets with high catastrophic collision probability usually take into account the flux density of crossing objects (for their current orbits), their cross sectional area and their mass, among other parameters [5]. With this in mind, R/Bs are at the top of the risk list, as they represent approximately 46% of the total mass in LEO, which is one of the most populated areas in the near-Earth region [6].

2.1 Distribution of rocket bodies

At the time of writing (i.e., 1st June, 2015), the total number of R/Bs in orbit is 2024. The major contributor in Europe to the R/B population is the Ariane family. Table 1 indicates their distribution in LEO, Medium Earth Orbit (MEO) and High Earth Orbit (HEO).

Object	Low Earth Orbit h<2000 km	Medium Earth Orbit 2000<h<35766 km	High Earth Orbit h>35766 km
Ariane-5 R/B	2	61	1
Ariane R/B	11	117	2
All R/B	790	1085	149

Table 1: Distribution of rocket bodies in Low, Medium and High Earth Orbit (where h is the altitude of a R/B) (information retrieved on 1st June, 2015 from the following sources [7, 8]).

2.2 Future trend and Active Debris Removal

The unabated growth of the space debris population has necessitated the introduction of new design guidelines for space missions [9, 10, 11]. However, Post-Mission Disposal (PMD) needs to be combined with ADR to stop future population growth. The optimum number of objects to be removed from orbit will depend on several parameters [12]. Nevertheless, the recommended number varies from 3 to 15 per year [5, 6, 13].

The first ADR mission targeting a non-cooperative object is planned to be carried out in 2021 by the European Space Agency (ESA) [14]. However, ADR involves a great number of challenges that still need to be proven in space. A review of ADR methods and main phases of an ADR mission can be found in the following articles: [14, 15, 16]. The most mature methods in terms of Technology Readiness Level (TRL) are those involving orbital robotics, since some of the technologies and techniques have been tested in orbit in the past.

3 STATE-OF-THE-ART IN ROBOTIC RENDEZVOUS AND CAPTURE

The first concept of an unmanned robotic spacecraft being employed for on-orbit servicing and assembly appeared as early as 1981, in a NASA report, as consequence of successful usage of the *Shuttle Remote Manipulator System* (SRMS) or *Canadarm* in the Space Shuttle program [17]. However, it was only sixteen years later that this idea turned into reality with the first-ever, unmanned robotic spacecraft with the *Engineering Test Satellite* (ETS)-*VII*. Prior to ETS-*VII*, the only spacecraft with a robotic manipulator were the space shuttle orbiters.

Several space missions have been launched with the goal of demonstrating technologies that overcome the limitations of remotely-controlled systems, such as the SRMSs. In addition, there are missions planned in the near future that will enable these technologies to be tested further. In this section, we provide a brief summary of important past and future missions.

The first one in chronological order is the ETS-VII mission, developed by the National Space Development Agency (NASDA) of Japan. Launched in 1997 with the purpose of testing robotic technologies in space and prove the feasibility of an unmanned on-orbit servicing (OOS), the mission achieved the first milestone in unmanned orbital robotics, despite a few mission hiccups [18].

The *Orbital Express* (OE) mission represents another important milestone in unmanned orbital robotics. It was developed by the US Defense Advanced Research Projects Agency (DARPA) and was launched in 2007. During the ninety days of the mission, objectives similar to the ETS-VII mission were successfully accomplished, but with a higher degree of autonomy. However, also in this case an anomaly in the flight software threatened the success of the whole mission [19, 20].

It is worth noting at this point that none of those missions dealt with a non-cooperative, tumbling target. Moreover, almost all of the missions mentioned here experienced malfunctions and anomalies to some degree[20]. Thus, it can be argued that much still needs to be done in this domain if robotic ADR is to become a routine operation. Future demonstration missions such as DARPA's Phoenix and DLR's DEOS represent a step forward in that direction.

The goal of the DARPA's Phoenix mission is to develop and demonstrate robotic technologies for capturing, harvesting and re-purposing valuable components (e.g. an antenna aperture) of a decommissioned GEO satellite. The first demonstration mission of one part of the space system, the "satlet", was scheduled for the third quarter of 2015 [21, 22, 23]. No information on the current status of this demonstration is publicly available at the time of writing.

Deutsche Orbitale Servicing mission (DEOS) is instead a more "traditional" mission, in line with ETS-VII and OE. Its goals are to demonstrate technologies and techniques for an unmanned on-orbit

robotic capture of a tumbling target[1] and its subsequent servicing. The mission is being developed by the German Aerospace Agency (DLR) and is scheduled for launch in 2018 [24].

4 AGORA MISSION

In this paper, we consider the Agora mission and develop the RVC architecture based on the top-level requirements and design constraints pertaining to this concept. We present a synopsis of an on-going Phase 0 study, geared at establishing the feasibility of the Agora mission concept. Agora is a demonstration mission geared towards the development and in-orbit testing of technologies to actively remove an Ariane R/B using a contactless de-tumbling system, based on eddy currents, and a robotic grasping mechanism. The de-orbiting of the target body will be performed in a controlled manner using a de-orbiting kit. The kit is attached to the target by the chaser spacecraft, which subsequently disengages. This provides an opportunity to scale the mission in the future to a multi-target scenario by including multiple de-orbit kits on the chaser. The envisioned mission will be performed in line with past and future robotic missions, according to the "craw, walk and run" paradigm [25], by gradually increasing its complexity as the preceding phases are successfully completed.

Since ADR has not yet been successfully demonstrated on-orbit, Agora is intended to serve as a stepping stone towards realizing the goal of removing harazardous R/Bs in the near future. With this in mind, the mission architecture is based around the concept of targeting the Ariane 5 upper stage used to place the Agora chaser on-orbit. This provides us with an opportunity to ensure that experiments can be conducted on-orbit whilst minimizing the risk of adding to the debris population in case of failure, given that R/B can use its own propulsion to perform the de-orbit if necessary.

4.1 Target object

The target object is the Storable Propellant Stage (EPS) of the Ariane 5 launcher, which will place the chaser spacecraft on the target orbit. This upper stage has a dry mass of 4550 kg, a diameter of 5.405 m and a length of 3.356 m [26]. It comprises a reignitable Aestus engine, propellant tanks and a vehicle equipment bay (VEB).

4.2 Chaser Spacecraft

The chaser is a robotic spacecraft, illustrated in Figure 1. Its main features are: a deployable, semi-rigid clamping mechanism, a de-tumbling device, a de-orbiting kit and a robotic arm. Its main characteristics are: (a) total mass of 2500 kg[2], (b) total power consumption of 709 W, (c) bus dimensions of $4.05(\text{L}) \times 3.3(\text{D})$ m, (d) fully deployed configuration dimensions of $7.41(\text{L}) \times 21.22(\text{W}) \times 7.76(\text{W})$ m, (e) total volume of 25.78 m^3.

The semi-rigid clamping mechanism is used exclusively for the capture of the target object after it has been de-tumbled. The capture is envisioned to occur on the plane that is as close as possible to the position of the center of gravity (COG) of the target, perpendicular to its "vertical" axis of symmetry. Its design was inspired by a finger of a hand of a humanoid robot and thus, it can be stowed during the launch, reducing the volume needed inside the fairing. Each finger is estimated to have a maximum length of 3.36 m, maximum width of 0.62 m and mass of around 36 kg. The total estimated mass of the device is around 96 kg.

The de-tumbling device consists of five magnetic coils placed around the main bus of the spacecraft (see Figure 1). The system is based on 2nd generation High Temperature Superconducting (HTS) wires and will be actively cooled using Loop Heat Pipes (LHPs) and cryocoolers. The total mass of the system[3] is estimated to be around 47 kg, while the required peak of power of the most power hungry component of the system, the cryocooler, is estimated to be around 250 W.

The chaser will carry a solid propellant, single-pulse kit similar to the one described in [27], consisting of a self-contained system capable of de-orbiting a target object with a single burn. The device will be stowed in the cavity of the chaser bus for the majority of the mission and will be attached inside the nozzle of the main engine of the R/B in a controlled manner by the robotic arm. The total estimated mass of the de-orbiting kit is around 130 kg.

[1] Tumbling at a rate of 4 deg/sec.

[2] Of which 2000 kg is the dry mass of the spacecraft (including 20 % margin and the mass of the launch adaptor) and 500 kg is the propellant mass.

[3] Considered in this paper as composed of the coils and supporting structure.

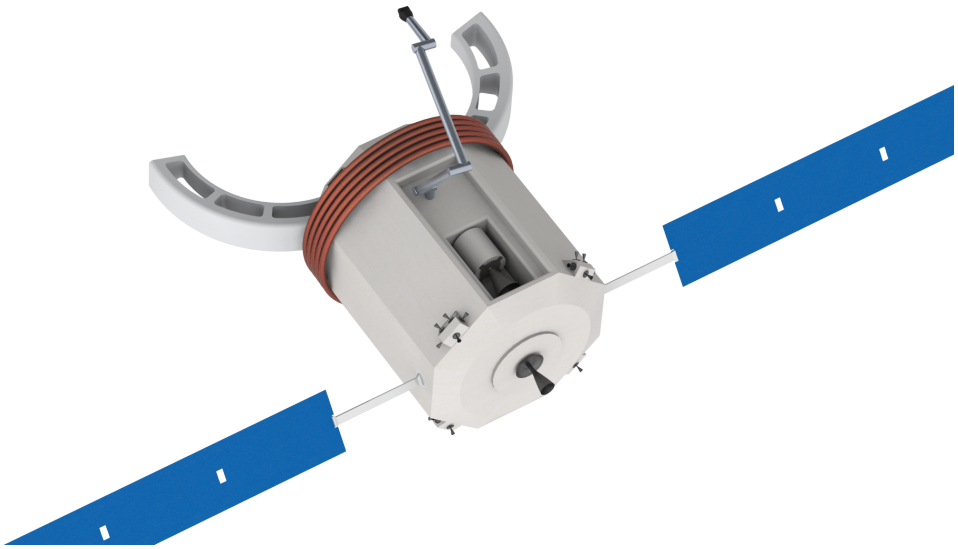

Figure 1: Chaser spacecraft concept

The robotic arm is employed for inspection purposes and placement of the de-orbiting kit. Its design is envisioned to be inherited from the one currently being developed for the DEOS mission [28], thus consisting of a 7 DOF, torque-controlled, lightweight manipulator, with a total mass of 54.6 kg and length of 5.25 m, measured from its base to the tip of its end-effector.

The chaser spacecraft is a three-axis stabilized vehicle by the means of: 24 ON/OFF bi-propellant attitude control thrusters (ACTs) (22 N thrust each) and four Control Moment Gyros (CMGs). The choice for CMGs was driven mainly by the need to reduce the usage of the ACTs during the operation of the de-tumbling device and control of the robotic arm. Moreover, future robotic ADR missions will most likely employ multi-target architectures, thus the usage of CMGs will be mandatory to reduce fuel requirements. In the end, the choice of CMGs instead of reaction wheels (RWs) was dictated also by the magnitude of the expected attitude disturbance on the base spacecraft that can not be handled by commercial RWs. A single, bi-propellant Orbital Control Thruster (OCT) (400 N thrust) provides the spacecraft with the capability to de-orbit itself at the end of the mission.

The spacecraft is equipped with sensors typical of a generic space mission, plus a suite of sensors needed for the execution of proximity operations and capture of the target. The former includes: coarse Earth and Sun sensors, three star sensors, three Inertial Measurement Units (IMUs) and one Global Positioning System (GPS) receiver. The latter on the other hand includes: two infrared (IR) and two optical cameras (for far and close-range rendezvous phases respectively), two scanning Light Detection and Ranging (LIDAR) sensors (for precise pose[4] estimation of the target) and one pair of stereo cameras (for the inspection and manipulation of the target object) [20].

4.3 Mission Phases

The nominal mission scenario for Agora consists of a robotic chaser spacecraft rendezvousing with, and capturing the target R/B. In particular, after the launch phase, it is expected that the chaser and target will find themselves separated by tens of kilometers, but in the same orbital plane, thus eliminating the need for phasing. The primary proximity phases include the following:

1. **Far-range rendezvous phase:** the chaser spacecraft will reduce the relative distance between itself and the target from kilometers down to a few hundreds of meters, in order to meet the requirements for the close-range rendezvous phase composed of the following sub-phases.

2. **First fly-around phase:** the pose of the target will be estimated and a visual inspection of the target will take place.

3. **De-tumbling phase:** the tumbling rates of the target will be reduced below a specified threshold using an enhanced magnetic field generated by on-board coils from a distance of tens of meters.

[4] Considered here as the position and orientation of an object.

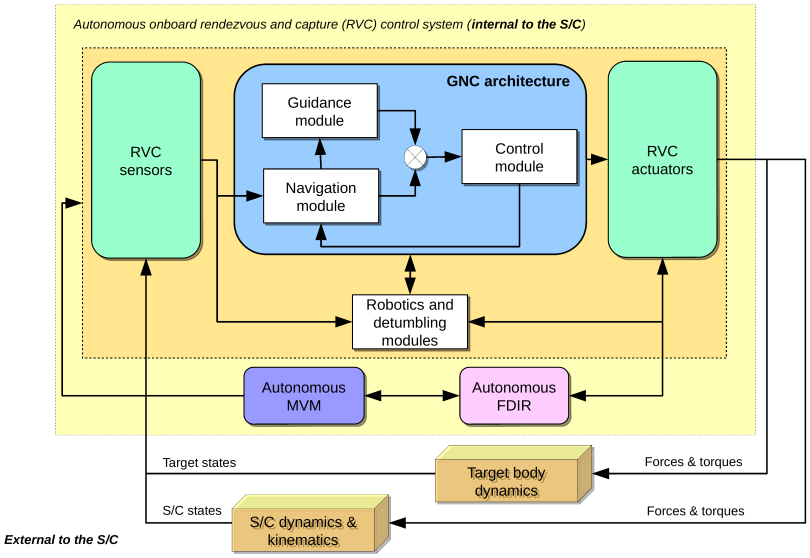

Figure 2: Autonomous on-board rendezvous and capture control system architecture [20]

4. **Attitude estimation phase (2nd fly around phase):** the attitude state of the target will be determined once again, to verify that the tumbling motion about all three axes satisfies the maximum specified threshold.

5. **Approach phase:** the chaser spacecraft will gradually approach the target, reducing the relative distance down to a few meters with full contingency measures in place.

6. **Capture and stabilization phase:** a semi-rigid clamping mechanism will be used to capture the target object, while dumping any residual relative motion. The Attitude Control System (ACS) will be used in this phase to actively stabilize the composite system.

7. **De-orbit kit insertion phase:** a robotic arm will be deployed and used to manipulate and insert the de-orbiting kit inside the nozzle of the main engine of the target.

8. **Disengagement phase:** after installation of the de-orbiting kit, the chaser spacecraft will reorient the composite system to the required position and orientation and will disengage from the target, retreating to a safe distance.

9. **De-orbiting phase:** the de-orbiting kit will be ignited and will carry out controlled re-entry of the target object. Afterwards, the chaser spacecraft will reorient itself and de-orbit itself using its own OCT.

5 RENDEZVOUS AND CAPTURE CONTROL SYSTEM

The RVC control system presented in this paper is a system responsible for [20]: (1) measuring the relative state of the target object with respect to the chaser spacecraft, (2) processing that information, (3) planning the execution of maneuvers and (4) executing them. The RVC control system manages all of these functions while guaranteeing the failure detection and isolation of anomalies and recovery of the system. Thus, we represent the architecture of the RVC system as a collection of modules and relationships between them (see Figure 2) [20]. The main modules of the architecture are: (a) navigation, (b) guidance, (c) control, (d) de-tumbling, (e) robotics, (f) Mission Vehicle Management (MVM) and (g) Failure Detection, Isolation and Recovery (FDIR)[5]. Each module includes software responsible for a particular task within the system [20]. The main properties of the architecture are modularity and flexibility. More about each module can be found in what follows, bearing in mind the requirements and constraints of the specific mission phases for Agora, summarized in Section 4.3.

[5]Please note that the last two modules, although within the envisioned RVC control system, are not presented in this paper.

5.1 Navigation Module

The navigation module is responsible for providing the current, estimated pose (position and orientation) vector to the guidance and control modules, through use of a filter [29]. For this study, the sensors used by the navigation module are: two LIDARs [30], to generate a precise 3D reconstruction of the target geometry and its pose, and a set of cameras (optical and IR), to provided vision-based data. Moreover, classical Attitude Determination and Control System (ADCS) sensors, such as IMUs, are also used to eliminate the ambiguity between pure rotation and translation [31]. In addition, due to output drift, the IMU sensors will need to be updated regularly by using measurements from extero-receptive sensors (i.e., Earth, Sun, or Star sensors) [29].

The reason for choosing LIDARs is due to their precision [32] and robustness to the conditions of the space environment. However, they have some drawbacks like: high power consumption, minimum range limitation, due to their small field of view, and the ability to cope with reflective surfaces. Thus, a combination between LIDARs and another set of sensors will be utilized during certain mission phases like the de-tumbling operations. The combination of LIDAR, optical and infrared cameras for semi-autonomous rendezvous and docking has been tested successfully on-orbit previously with systems such as TriDAR [33]. Agora will adopt a similar approach to ensure that operations can be conducted safely in a variety of illumination conditions and mission phases. Moreover, a combination of two LIDARS should guaratnee more precision in the pose estimation of the target and thus a very strict ADCS uncertainty box necessary to successfully capture the target with the semi-rigid clamp [14].

The selected filters for the navigation module are the Extended Kalman filter (EKF) and the Unscented Kalman filter (UKF). Both filters are robust attitude estimators that should provide fast convergence, robustness and stability in the whole state-space of the mission, although their convergence and robustness can not be guaranteed a priori as in case of a traditional Kalman filter [18].

5.2 Guidance Module

The guidance module provides the reference values for the state vector at each time step and includes a description of planned actuation maneuvers, e.g., in terms of thrust vector and duration [29]. In particular, the guidance module should provide position and attitude profiles, as a function of time, covering all the mission phases. These reference values represent the planned approach of the chaser through all the phases of the Agora mission and are computed based on an optimization of the chosen parameters, like ΔV (proxy for the total fuel consumption of the spacecraft). For the Agora mission, we foresee a number of key requirements that determine the boundary conditions for the design of the guidance module.

The far-range rendezvous phase is well understood in general [34], having been studied extensively for many rendezvous scenarios that have been successfully executed on-orbit. Our baseline design is based on adopting a similar strategy to the guidance system developed for the Automated Transfer Vehicle (ATV) [35].

For the close-range phases, a degree of autonomy will be required on-board to handle the knowledge gained about the target and the environment through acquisition of sensor data. Moreover, passive safety of the approach trajectory will also be required in order to ensure the safety of the spacecraft even in the event of its total shutdown. Thus, an entry corridor will be defined. This corridor will demark a strict set of boundary conditions that will enable a Mixed-Integer Linear Programming (MILP) algorithm or similar to be employed [36]. In particular, the linear formulation of the algorithm described in [36] can cope with the optimization problem, while at the same time being seven times more efficient then a strict straight line approach [36]. An uncertainty sphere will also be adopted in the optimization process, to ensure that passive safety is included as a feature of the approach trajectory, in case the entry corridor is exceeded.

5.3 Control Module

The control module is responsible for providing the commands (i.e., control forces and torques) to correct the deviations of the actual pose vector from the desired one. Additionally, it has to ensure the stability of the spacecraft and suppress external disturbances [29].

Reflecting upon the mission phases outlined in Section 4.3, it becomes apparent the the control system must handle a large range of scenarios. However, all of them can be grouped under two major control strategies: Single-Input-Single-Output (SISO) and Multiple-Input-Multiple-Output (MIMO), depending on the distance from the target. The first one is to be used for all mission phases where the relative

distance between the chaser and target is greater than 50 m, while the second one is to be used in all the other phases. In fact, at distances greater then 50 m, translational and rotational motions of the chaser spacecraft can be controlled separately due to their relatively weak coupling. However, at closer distances this can not be considered as valid anymore and a contemporaneous control of the translational and rotational dynamics needs to be taken into account [20, 37, 29]. Thus, the major requirements of a controller are its stability, robustness and ability to optimize multiple variables.

The selected algorithms for the control module are the Proportional-Integral-Derivative (PID) and Linear-Quadratic Regulator (LQR). The PID is a well-known controller and, although it is not capable of solving the optimization problem, it is a robust algorithm; hence, it will be used as baseline in the early phase of the study. The LQR, on the other hand, will be used later on in this study as a more advanced controller capable of multi-variable optimization [20].

5.4 De-Tumbling Module

The de-tumbling device, as its name implies, is used to actively de-tumble the target using the 'Eddy Brake' method, based on the generation of the eddy currents on the target body by the magnetic field generated by the chaser spacecraft [38]. Analysis of the dynamics of the 'Eddy Brake' method is a challenging problem, since it involves the coupling of the linear and rotational dynamics of both the chaser and target objects during the de-tumbling process. Moreover, due to the magnetic interactions between the two objects, the chaser will be subject to torques and forces, which need to be taken into account by the ADCS and counteracted. With this in mind, the main requirements for the GNC subsystem during the de-tumbling process are to maintain a: (a) fixed relative distance between the chaser and target, (b) fixed relative pointing between the coil and the target object, (c) fixed inertial position of the chaser spacecraft once it has acquired an appropriate relative pose.

The first requirement demands a fixed distance between the two objects. The magnetic field is inversely proportional to the cube of the distance, which means that the process will be more efficient the closer the two objects are. As a baseline for this study, a relative distance of 10 m, between the coil and the COG of the target object, has been selected. In addition, variations in the distance should be avoided. In fact, a sudden increase of the distance would result in a decay of the field at the COG of the target, which would lead to a net attractive force between the two objects. Analogously, if the chaser suddenly approaches the target object, this would result in a repulsive force between the two objects [39].

The second requirement mandates fixed relative pointing between the coil and the target object, which implies that the chaser must counteract external torques during operations. The two main expected perturbations are the eddy current torque, induced by the magnetic interaction between the two objects, and the torque due to the interaction of the coil with the Earth's magnetic field. The latter perturbation will tend to align the magnetic dipole of the coil with the Earth's magnetic field. The baseline orbit for the Agora mission lies at an altitude of 500 km, thus it can be concluded that the torque induced by the Earth's magnetic field exceeds the eddy current torque by several orders of magnitude. As a baseline, CMGs have been selected to counteract this perturbation. An alternative solution, which is still under research, is to make use of an alternating current. This would lead to a null perturbing torque on the coil during each cycle of the AC current and no additional forces between the two objects would appear for the same reason.

The relative pointing of the coil is of paramount importance in order to optimize the de-tumbling process. If the magnetic field induced at the COG of the target is parallel to the angular velocity vector, the eddy current torque will be zero [38]. Therefore, to maximize the torque induced on the target, the magnetic dipole of the coil should be perpendicular to the angular velocity of the target object. This leads to two important consequences:

- A pose estimation process needs to be carried out during the de-tumbling process in order to estimate the 'Euler axis' of the target object for feedback control.
- The chaser spacecraft may need to change its relative orientation with respect to the target object, in order to damp all three angular components of the target's tumbling motion.

The third requirement necessitates a fixed inertial position of the chaser spacecraft once it has acquired an appropriate relative pose, in order to achieve a constant de-tumbling effect on the target. In fact if only the relative pose is controlled, the angular rotation of the target would transfer to the chaser and the two objects would start rotating around the COG of the chaser-target system until the the angular

velocities of the two objects are matched. In this situation, no eddy currents would be induced on the target object and the de-tumbling process would stop. However, this effect might be beneficial in the transition between the de-tumbling and the capture phases (see Section 4.3). In fact, once the desired angular velocity of the target has been achieved through active de-tumbling, the chaser will need to initiate the approach to, and capture of the target. During those phases, relative linear and angular rates between chaser and target will need to be below a certain threshold [29] and this is generally achieved by the means of the ACS. Thus, instead of using the ACS, the de-tumbling device could be used to achieve these conditions simply by not controlling the inertial position of the chaser described above.

An example of the necessary maneuvers of the chaser spacecraft to counteract the torques resulting from magnetic interactions between the coil and the target only (i.e., no environmental perturbations are considered) is illustrated in the following results of a numerical simulation. In the simulation carried out, the chaser and target are assumed to be moving in a 2D plane, xy, and to have uniaxial rotation about the perpendicular z-axis. The target object is modeled as a spherical shell with an initial angular velocity of $10\,{}^{\mathrm{deg}}/_{\mathrm{s}}$ and having the following mass properties: mass of 4500 kg and inertia of $20,600\,\mathrm{kg}\cdot\mathrm{m}^2$[6]. The total effective conductive mass considered for the de-tumbling process is equal to 7 % of the total mass of the target. Since the target is modeled as a sphere, all inertia axes are equal and are principal axes. The mass properties of the chaser spacecraft considered in the simulation are: mass of 2500 kg and inertia (along the z-axis) of $10,300\,\mathrm{kg}\cdot\mathrm{m}^2$. The de-tumbling process is carried out until the spin rate of the target is reduced below $3\,{}^{\mathrm{deg}}/_{\mathrm{s}}$ and a PID controller is employed for the execution of the maneuvers. Figure 3 and 4 show the results of the simulation. In particular, Figure 3 illustrates the evolution of the angular velocity of the target while Figure 4 depicts the evolution of the control maneuvers performed by the ACS of the chaser.

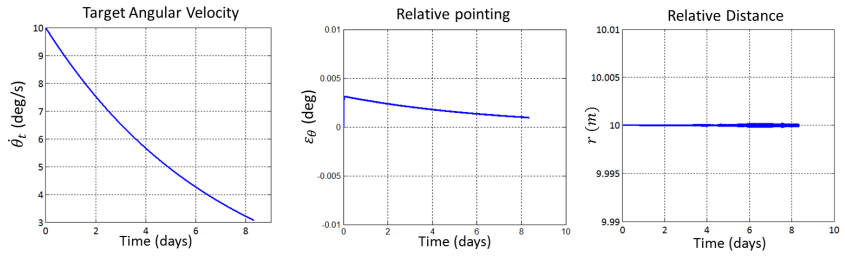

Figure 3: Evolution of angular velocities of the target, relative pointing and relative distance with respect to the chaser during simulation of de-tumbling process.

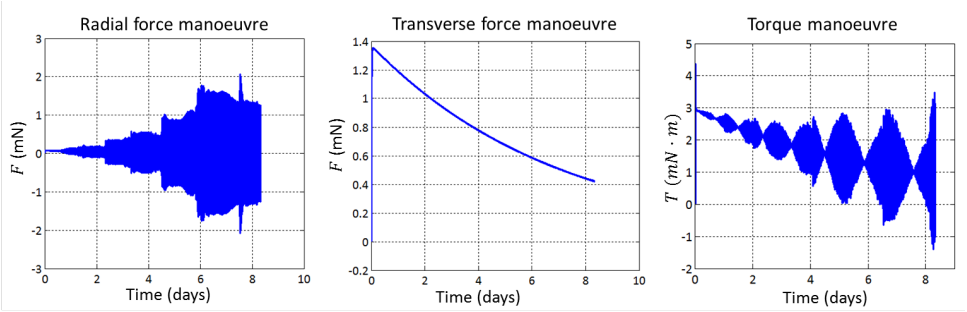

Figure 4: Evolution of the control maneuvers executed by chaser during simulation of de-tumbling process.

5.5 Robotics Module

The functions of the robotics module are: (a) capture of the target object with the clamping mechanism and (b) placement of the de-orbiting kit inside the nozzle of the main engine of the target. Both functions need to be performed, while at the same time minimizing the disturbance of the attitude of the base

[6]These values correspond to the mass properties of an EPS of the Ariane-5 launcher [26].

spacecraft, resulting from the dynamical coupling between the latter and the robotic devices. This effect is particularly evident during the manipulation of the de-orbiting kit, when the mass ratio between the base and the manipulator is equal to $35:1$[7]. For comparison, the mass ratio of the robotic arm before the manipulation of the de-orbiting kit is equal to $119:1$, while the one of the clamping mechanism is equal to $20:1$. The mass ratio between the manipulator and the chaser spacecraft only is instead equal to $36:1$. Moreover, the contact between the target and the augmented manipulator[8] needs to be compliant in order not to introduce impact forces and thus additional attitude disturbance to the base. The allowed attitude disturbance is defined by the spacecraft communication system[9] and it is safe to be assumed to be of the order of $1\,\mathrm{deg/s}$.

The decision to exclude the robotics module from the rest of the GNC architecture (visible in Figure 2) was driven by the desire to make the whole RVC system as modular as possible and to lower the computational requirements of the on-board computer. In fact, developing a control system for the entire spacecraft considered as one dynamical system could prove unfeasible due to the high number of DOF the system has. However, in this case the coordination between the ADCS of the spacecraft base and the manipulator is necessary [40]. With this in mind, two possible control strategies are envisioned for this mission: free-flying and free-floating. The former is based on feed-forward compensation of the attitude disturbance due to the movement of the arm, so that the base of the spacecraft can be considered fixed. The latter strategy, on the other hand, allows dynamical coupling between the base and manipulator, while the ADCS is active only to counteract external torques acting on the spacecraft (e. g. gravity gradient, air drag, etc.). It is obvious that the free-flying strategy allows simpler control of the manipulator. However, it requires higher energy consumption and generally leads to higher position and orientation errors of the end-effector (EE) of the manipulator, as demonstrated by the ETS-VII mission [41]. Thus, the free-floating strategy will be preferred in this mission. The capture and manipulation of the target object will be performed in a "supervised" mode, meaning that operators will monitor the execution of the tasks and intervene only in case of anomalies or unexpected behavior of the system.

The control algorithm of the clamping mechanism is straightforward, since its influence on the spacecraft attitude during its deployment is small and only simple open/close commands need to be imparted. This will be executed using a proportional-derivative (PD) controller until the fingers encounter the surface of the target object. At this point, the force applied by the fingers will increase and proportionally the current sent to the motor will increase until a predefined threshold. The system will then initiate a mechanical self-locking mechanism that will ensure that the system will not release the target object even in case of power cut-off. The reverse command will be performed for the release of the target.

The control strategy of the robotic arm is on the other hand more complex, especially in free-floating mode although it can be argued that due to the mass ration higher than $10:1$ a simple PID or even a PD controller can be employed [42] to control the arm in the approach phase. However, by using this control strategy an initial error of the EE is to be expected givn that the reaction of the base will be present also in this case [42]. Thus, to minimize the base reaction we have choosen a different control strategy consisting of two different control laws: impedance control and Distributed Momentum Control (DMC), used depending on the phase of the mission. More in detail, considering a robotic spacecraft, such as the Agora chaser, the angular momentum of the system can be written as follows [43]:

$$\boldsymbol{L} = \tilde{\boldsymbol{H}}_b \boldsymbol{\omega}_b + \tilde{\boldsymbol{H}}_{bm} \dot{\boldsymbol{\phi}}_m + \tilde{\boldsymbol{H}}_{br} \dot{\boldsymbol{\phi}}_r + \boldsymbol{r}_g \times \boldsymbol{P} \tag{1}$$

where $\boldsymbol{P}$ and $\boldsymbol{L}$ are the linear and angular momentum of the system, $\tilde{\boldsymbol{H}}_b$, $\tilde{\boldsymbol{H}}_{bm}$ and $\tilde{\boldsymbol{H}}_{br}$ are the components of the inertia matrices $\boldsymbol{H}_b$ and $\boldsymbol{H}_c$, respectively, defined in [44] as the augmented inertia matrix of the base and augmented coupling inertia matrix, $\boldsymbol{\omega}_b$, $\dot{\boldsymbol{\phi}}_m$, $\dot{\boldsymbol{\phi}}_r$, and $\boldsymbol{r}_g$ are the angular velocity of the base, joint velocities of the manipulator and CMGs, and the position of the center of gravity of the robotic system with respect to the inertial reference frame[10], respectively.

The manipulator kinematics can be described as [43]:

$$\begin{bmatrix} \boldsymbol{v}_h \\ \boldsymbol{\omega}_h \end{bmatrix} = \boldsymbol{J}^* \begin{bmatrix} \dot{\boldsymbol{\phi}}_m \\ \dot{\boldsymbol{\phi}}_r \end{bmatrix} + \dot{\boldsymbol{x}}_{gh} \tag{2}$$

where $\boldsymbol{v}_h$ and $\boldsymbol{\omega}_h$ are the linear and angular velocity of the EE of the manipulator, $\boldsymbol{J}^* = \begin{bmatrix} \boldsymbol{J}_m^* & \boldsymbol{J}_r^* \end{bmatrix}$

[7] Considering the mass of the base equal to $6365.4\,\mathrm{kg}$, i. e., equal to the dry mass of the chaser spacecraft plus that of the target body minus the masses of arm and de-orbiting kit

[8] Defined as combination of the manipulator and the de-orbiting kit attached firmly to its end-effector.

[9] Or more precisely by the antenna pointing error

[10] Defined as the orbital or "roll-pitch-yaw" frame

is the *generalized Jacobian matrix* (GJM), while $\dot{\boldsymbol{x}}_{gh}$ is the velocity of the center of gravity of the robot projected onto the velocity of the EE.

With the previous equations in mind, the DMC of a redundant space manipulator, such the one of the Agora spacecraft, can be defined as [43]:

$$\dot{\boldsymbol{\phi}}_m^d = \tilde{\boldsymbol{H}}_{bm}^+(\boldsymbol{L}_g - \tilde{\boldsymbol{H}}_{br}\dot{\boldsymbol{\phi}}_r) + \boldsymbol{P}_{RNS}\boldsymbol{\xi} \tag{3}$$

where $\dot{\boldsymbol{\phi}}_m^d$ is the desired manipulator joint velocity, $^+$ indicates the pseudo-inverse matrix, $\boldsymbol{L}_g$ is the total angular momentum of the robot around its center of gravity, $\boldsymbol{P}_{RNS} = \boldsymbol{E}_m - \tilde{\boldsymbol{H}}_{bm}^+\tilde{\boldsymbol{H}}_{bm}$ is the projector onto the null space of $\tilde{\boldsymbol{H}}_{bm}$ and $\boldsymbol{E}_m$ is the identity matrix. $\boldsymbol{\xi}$ is a vector defined as [43]:

$$\boldsymbol{\xi} = (\boldsymbol{J}_m^*\boldsymbol{P}_{RNS})^+[\boldsymbol{x}_h^d - \boldsymbol{J}_r^*\dot{\boldsymbol{\phi}}_r - \dot{\boldsymbol{x}}_{gh} - \boldsymbol{J}_m^*\boldsymbol{H}_{bm}^+(\boldsymbol{L}_g - \tilde{\boldsymbol{H}}_{br}\dot{\boldsymbol{\phi}}_r)] \tag{4}$$

where $\boldsymbol{x}_h^d$ represents a desired position and orientation of the EE in inertial reference frame.

In the end, the impedance control law of the free-floating robot can be defined as [43]:

$$\dot{\boldsymbol{\phi}}_m^d = \boldsymbol{J}_m^{*+}(\boldsymbol{x}_h^d - \boldsymbol{J}_r^*\dot{\boldsymbol{\phi}}_r - \dot{\boldsymbol{x}}_{gh}) \tag{5}$$

Thus, if the augmented manipulator is used to approach the target nozzle, the DMC is used, otherwise, just before the contact phase, the impedance control is employed. This way the approach phase is performed in such a way that the attitude disturbance of the base is minimized, while during the contact phase impedance matching is guaranteed [43]. In all other cases[11], a simple PID control of the robotic arm is enough to perform the task due to a big mass ratio between the base and the arm. On the path planning side, at the moment (for the sake of the simplicity) a simple Cartesian point-to-point path planning is envisioned during all robotic phases. The relative pose estimation of the EE of the manipulator and the target or other objects is assumed to be performed by the GNC and through the usage of the stereo-cameras mounted on the manipulator itself.

6 CONCLUSIONS AND FUTURE WORK

The space debris population has grown significantly over the last two decades, especially in LEO, and recent studies indicate that it will continue to grow in the future, leading soon enough to a belt of debris in certain regions that could present a significant hazard to future space missions. Thus, the time might have come to consider ADR as a serious option for stabilizing the space debris environment.

Within this context, in this paper, we present the concept of the robotic Agora mission with particular focus being given to the concept of the RVC control architecture needed to safely de-tumble, capture and manipulate the target object. In particular, in this paper, we have provided an overview of the top-level requirements of the mission and brief descriptions of the target and the chaser spacecraft. Moreover, key mission phases are described given their influence on the design of the RVC control architecture. In the end, individual modules of the RVC control system are presented, outlining the general requirements for each one of them and stating the envisioned algorithms that will be implemented in the near future. Particular attention in the paper is given to the de-tumbling and robotics modules, given their significant impact on the RVC control architecture as a whole.

Future work includes the definition of the MVM and FDIR modules of the architecture that will contribute to the autonomous character of the system. Moreover, the software implementation and testing of the outlined architecture will be performed in the near future to investigate and validate the desired capabilities of the envisioned robotic spacecraft.

ACKNOWLEDGMENTS

The research work here presented is developed as part of the European Union Framework 7 Program, Marie Curie Initial Training Networks (ITN) project 'Stardust' [45]. Thus, the authors would like to thank the European Commission and the Research Executive Agency for their support and funding.

[11] Like during the inspection phase.

References

[1] J.-C. Liou, N. Johnson, and N. Hill, "Controlling the growth of future LEO debris populations with active debris removal," *Acta Astronautica*, vol. 66, no. 5-6, pp. 648–653, Mar. 2010.

[2] D. J. Kessler and B. G. Cour-Palais, "Collision frequency of artificial satellites: The creation of a debris belt," *Journal of Geophysical Research*, vol. 83, no. A6, pp. 2637–2646, June 1978.

[3] ESA, "Clean space programme," Online, 2013. [Online]. Available: http://www.esa.int/

[4] F. LaPorte and E. Sasot, "Operational Management of Collision Risks for LEO Satellites at CNES," in *AIAA SpaceOps Conference*. AIAA 2008-3409, 2008.

[5] H. Klinkrad, "The Space Debris Environment and its Evolution," in *6th IAASS Conference*, Montreal, Canada, May 2013.

[6] J.-C. Liou, "An active debris removal parametric study for LEO environment remediation," *Advances in Space Research*, vol. 47, no. 11, pp. 1865–1876, June 2011.

[7] ESA, "Discos (database and information system characterising objects in space)," Online, 2015. [Online]. Available: http://www.esa.int/

[8] Scitor under contract to JFCC SPACE/J3, "Space-track website." Online, June 2015. [Online]. Available: https://www.space-track.org

[9] ESA, "Position Paper on Space Debris Mitigation. Implementing Zero Debris Creation Zones," European Space Agency, The Netherlands, Tech. Rep. SP-1301, 2005.

[10] NASA, "Process for Limiting Orbital Debris," National Aeronautics and Space Administration, Washington, DC, USA, Tech. Rep. NASA-STD-8719.14A, 2011.

[11] UNOOSA, "Active debris removal - an essential mechanism for ensuring the safety and sustainability of outer space," Committee on the Peaceful Uses of Outer Space, United Nations Office for Outer Space Affairs, Vienna, AT, Tech. Rep. A/AC.105/C.1/2012/CRP.16, February 2012.

[12] A. E. White and H. G. Lewis, "An adaptive strategy for active debris removal," *Advances in Space Research*, vol. 53, pp. 1195–1206, April 2014.

[13] L. G. Hugh, A. E. White, R. Crowther, and H. Stokes, "Synergy of debris mitigation and removal," *Acta Astronautica*, vol. 81, pp. 62–68, December 2012.

[14] R. Biesbroek, T. Soares, J. Huesing, K. Wormnes, and L. Innocenti, "The e.deorbit cdf study: a design study for the safe removal of a large space debris," in *64th International Astronautical Congress (IAC)*, Beijing, September 2013.

[15] K. Wormnes, R. Le Letty, L. Summerer, H. Krag, R. Schonenborg, O. Dubois-Matra, E. Luraschi, J. Delaval, and A. Cropp, "ESA technologies for space debris remediation," in *6th European Conference on Space Debris*. Darmstadt, Germany: ESA, April 2013, pp. 1–2.

[16] C. Bonnal, J.-M. Ruault, and M.-C. Desjean, "Active debris removal: Recent progress and current trends," *Acta Astronautica*, vol. 85, pp. 51–60, April–May 2013.

[17] K. Yoshida and B. Wilcox, "Space robots and systems," in *Springer Handbook of Robotics*, B. Siciliano and O. Khatib, Eds. Berlin, Heidelberg, Germany: Springer Berlin Heidelberg, 2008, ch. 45, pp. 1031–1063.

[18] S. Nolet and D. W. Miller, "Development of a Guidance , Navigation and Control Architecture and Validation Process Enabling Autonomous Docking to a Tumbling Satellite," PhD Thesis, Massachusetts Institute of Technology, Cambridge, MA, USA, June 2007.

[19] K. Yoshida, "Achievements in space robotics," *Robotics & Automation Magazine, IEEE*, vol. 16, no. 4, pp. 20–28, December 2009.

[20] M. Jankovic, J. Paul, and F. Kirchner, "Gnc architecture for autonomous robotic capture of a non-cooperative target: preliminary concept design," *Advances in Space Research*, May 2015.

[21] P. Melroy, "Phoenix," Online, June 2012. [Online]. Available: http://goo.gl/XGGBek

[22] C. G. Henshaw, "The DARPA Phoenix Spacecraft Servicing Program: Overview and Plans for Risk Reduction," in *Proceedings of the 12th International Symposium on Artificial Intelligence, Robotics and Automation in Space*, ESA ESTEC. Montreal, Canada: ESA ESTEC, June 2014.

[23] R. Courtland, "Darpa prepares to launch "satlets"," Online, December 2014. [Online]. Available: http://goo.gl/JbiSpH

[24] Airbus Defence & Space, "Astrium wins DEOS contract to demonstrate in-orbit servicing," Online, September 2012. [Online]. Available: http://goo.gl/VwaWx5

[25] F. Sellmaier, T. Boge, J. Spurmann, S. Gully, T. Rupp, and F. Huber, "On-Orbit Servicing Missions: Challenges and Solutions for Spacecraft Operations," in *SpaceOps 2010 Conference*, no. AIAA 2010-2159. Huntsville, Alabama, USA: AIAA, April 2010, pp. 1–11.

[26] F. Hauss, "Ariane-5. Data relating to Flight VA213," Arianespace, Kourou, French Guiana, Tech. Rep., June 2013.

[27] D-Orbit Inc., "D-Orbit Product List," Online, 2015. [Online]. Available: http://goo.gl/ZRyNHr

[28] D. Reintsema, B. Sommer, T. Wolf, J. Theater, A. Radthke, J. Sommer, W. Naumann, and P. Rank, "DEOS: The In-flight Technology Demonstration of German's Robotics Approach to Dispose Malfunctioned Satellites," in *11th Symposium on Advanced Space Technologies in Robotics and Automation (ASTRA2011)*. Noordwijk, Netherlands: ESA, May 2011.

[29] W. Fehse, *Automated Rendezvous and Docking of Spacecraft*, 2009th ed., ser. Cambridge Aerospace Series, M. J. Rycroft and W. Shyy, Eds. New York, USA: Cambridge University Press, October 2003, no. 16.

[30] J. A. Christian and S. Cryan, "A Survey of LIDAR Technology and its Use in Spacecraft Relative Navigation," *AIAA Guidance Navigation and Control Conference*, pp. 1–7, 2013.

[31] E. Kervendal, T. Chabot, and K. Kanani, "GNC Challenges and Navigation Solutions for Active Debris Removal Mission," in *Advances in Aerospace Guidance, Navigation and Control*, Q. Chu, B. Mulder, D. Choukroun, E.-J. van Kampen, C. de Visser, and G. Looye, Eds. Springer Berlin Heidelberg, 2013, pp. 761–779.

[32] F. Kennedy, "Orbital Express," Online, Orlando, Florida, USA, pp. 3, 4, 11, 12, 17, 18, 2008.

[33] S. Ruel, T. Luu, and A. Berube, "Space shuttle testing of the TriDAR 3D rendezvous and docking sensor," *Journal of Field Robotics*, vol. 29, no. 4, pp. 535–553, July-August 2012.

[34] G. Di Mauro, "Theory and Experiments on Nonlinear Control for Space Proximity Maneuvers," PhD Thesis, Politecnico di Milano, Milan, Italy, Milano, Italy, March 2013.

[35] D. Pinard, S. Reynaud, P. Delpy, and S. E. Strandmoe, "Accurate and autonomous navigation for the ATV," *Aerospace Science and Technology*, vol. 11, no. 6, pp. 490–498, September 2007.

[36] L. S. Breger and J. P. How, "Safe Trajectories for Autonomous Rendezvous of Spacecraft," *Journal of Guidance, Control, and Dynamics*, vol. 31, no. 5, pp. 1478–1489, September–October 2008.

[37] Y. Luo, J. Zhang, and G. Tang, "Survey of orbital dynamics and control of space rendezvous," *Chinese Journal of Aeronautics*, vol. 27, no. 1, pp. 1–11, Feb. 2014.

[38] N. Ortiz Gómez and S. J. Walker, "Eddy Currents applied to De-tumbling of Space Debris: Analysis and Validation of Approximate Proposed Methods," *Acta Astronautica*, vol. 114, pp. 34–53, April 2015.

[39] B. Z. Reinhardt, B. Hencey, and M. Peck, "Characterization of eddy currents for space actuation," in *AIAA/AAS Astrodynamics Specialist Conference, Minneapolis, Minnesota.*, August 2012.

[40] M. Oda and Y. Ohkami, "Coordinated control of spacecraft attitude and space manipulators," *Control Engineering Practice*, vol. 5, no. 1, pp. 11–21, January 1997.

[41] K. Yoshida, "Engineering Test Satellite VII Flight Experiments for Space Robot Dynamics and Control: Theories on Laboratory Test Beds Ten Years Ago, Now in Orbit," *The International Journal of Robotics Research*, vol. 22, no. 5, pp. 321–335, May 2003.

[42] Y. Xu and H.-Y. Shum, "Dynamic control of a space robot system with no thrust jets controlled base," Robotics Institute, Pittsburgh, PA, US, Tech. Rep. CMU-RI-TR-91-33, August 1991.

[43] T. Oki, H. Nakanishi, and K. Yoshida, "Whole-body motion control for capturing a tumbling target by a free-floating space robot," in *2007 IEEE/RSJ International Conference on Intelligent Robots and Systems*. IEEE, Oct. 2007, pp. 2256–2261.

[44] Y. Xu and T. Kanade, Eds., *Space Robotics: Dynamics and Control*, 1st ed., ser. The Springer International Series in Engineering and Computer Science. Springer US, 1993, vol. 188.

[45] P. McGinty, "Stardust programme: Advanced research network on asteroid and space debris manipulation." Online, 2013. [Online]. Available: http://www.stardust2013.eu/